



Dual functional Fe/AC for treating phenol solutions by adsorption coupled with dry catalytic oxidation technology

Bingzheng Li^{a,*}, Huiyuan Wu^a, Chan Zhang^a, Wei Zheng^a, Dekui Sun^{b,*}, Shiwen Lei^c

^aSchool of Environment & Safety, Taiyuan University of Science & Technology, Taiyuan 030024, P. R. China, Tel. +86 351 6962589, Fax +86 351 6962600, email: bzli@tyust.edu.cn (B. Li), whywhywhy_95@163.com (H. Wu), zhang_chan@yahoo.com (C. Zhang), zhwwstar2016@163.com (W. Zheng)

^bState Key Laboratory of Coal Conversion, Shanxi Institute of Coal Chemistry, Chinese Academy of Sciences, Taiyuan 030001, P. R. China, Tel. +86 351 6962589, Fax +86 351 6962600, email: dksun@sxicc.ac.cn (D. Sun)

^cKey Laboratory of Carbon Materials, Shanxi Institute of Coal Chemistry, Chinese Academy of Sciences, Taiyuan 030001, P. R. China, email: leishiwen705@sxicc.ac.cn (S. Lei)

Received 12 September 2018; Accepted 16 June 2019

ABSTRACT

This work consists of preparation of iron-doping activated carbon (Fe/AC) by pore impregnation, the effects of $\text{Fe}(\text{NO}_3)_3$ treatment on the physical/chemical properties of activated carbon (AC), the effects of main influential experiment parameters such as contact time, initial phenol concentration, temperature and pH on adsorption of phenol onto AC and Fe/AC, the effects of various regeneration methods including thermal regeneration and dry catalytic oxidation on the adsorption capacity of AC and Fe/AC for phenol, the catalytic oxidation behaviors of phenol adsorbed over Fe/AC and the assessment of the adsorption capacity of Fe/AC for phenol in the adsorption-oxidation runs. The adsorbent-catalysts were characterized by liquid N_2 adsorption, scanning electronic micrograph, elemental analysis, Boehm titration, Fourier transform infrared spectroscopy and temperature-programmed desorption. To understand equilibrium adsorption, the adsorption data were analyzed by Langmuir, Freundlich, Dubinin-Radushkevich and Temkin models. To predict the nature of adsorption, the thermodynamic parameters (ΔG° , ΔH° and ΔS°) were calculated and analyzed. The results show that the $\text{Fe}(\text{NO}_3)_3$ treatment increases obviously the oxygenated acidic surface groups of AC. The equilibrium capacity of Fe/ACs for high-concentration phenol is lower than that AC. More surface acidic groups of Fe/AC decrease the equilibrium uptake of phenol and the order of the phenol uptake by the adsorbent-catalysts follows $\text{AC} > \text{Fe1/AC} > \text{Fe5/AC}$ mainly due to an increase in competition of water adsorption derived from the increase in surface hydrophilic property of AC or more water clusters formed in adsorption processes. Langmuir model can better describe adsorption of phenol on AC and low mass-fraction Fe-doping AC, whereas Freundlich model meets with that high mass-fraction Fe-doping AC. Adsorption of phenol on AC and Fe/AC is spontaneous and exothermic. Compared with original AC, Fe/AC has high catalytic oxidation performance of phenol on Fe/AC. Fe/AC shows higher phenol adsorption in successive runs. For pollution-free treatment, the dry catalytic oxidation of phenol is significantly superior to thermal regeneration. The experimental results indicate that dual functional Fe/AC can be used to effectively remove phenol from wastewater.

Keywords: Adsorption; Catalytic oxidation; Phenol; Fe/AC; Coupling

*Corresponding author.

1. Introduction

Low-concentration organic-wastewater-treating technology combining adsorption of organic pollutants from wastewaters with dry catalytic oxidation of the adsorbed pollutants over adsorbent-catalyst after the wastewater discharge (ADCO) has been a promising alternative for treatment of dilute wastewater streams containing highly toxic and/or non-degradable organic pollutants [1]. ADCO includes four consecutive procedures in a reactor: 1) liquid phase adsorption, 2) wastewater discharge, 3) catalytic oxidation, and 4) cooling (Fig. 1). Significantly, it is very important for adsorbent-catalysts in ADCO to have high adsorption capacity of organics in wastewaters and high catalytic oxidation performance of catalyst-adsorbed organic pollutants under dry condition. Usually, the catalysts used in ADCO can be classified into two types [2,3]: inorganic material-based catalysts (support: Al_2O_3 , SiO_2 , and activated species: individual metal oxide (CuO , Fe_2O_3) and multiple metal oxide) and the organic material-based catalyst, i.e., activated carbon-supported metal catalysts (metal/ACs). Due to its poor adsorption performance of aqueous organics, the former has been gradually abandoned, whereas more attention has been paid to the development of metal/ACs by the researchers [4–6].

Among these, due to their low cost, Cu and Fe or their oxides as catalytic activated species on AC were studied, e.g., our preliminary study [6] shows that both Cu/AC (copper-doping activated carbon) and Cu-Ce/AC (bimetal catalyst) have higher adsorption capacity and higher catalytic oxidation activity of phenol and aniline. Other studies about Fe and mixed Fe-containing catalysts also show that the element Fe of the catalysts has better catalytic performance of phenol and dyes [5–7]. But whether and how AC-supported Fe has an active or negative role in its phenol adsorption behaviors and its mechanism has not been thoroughly discussed yet. As we know, excellent organics adsorption performance is a prerequisite for the catalysts used in ADCO, and the adsorption capacity of AC-based catalysts frequently depends strongly on sup-

port AC. This uptake of organics by AC is derived from its structure and surface chemistry [8–13]. It should be noting that Fe doping process may influence the structure and/or surface chemistry of AC, and accordingly it may change adsorption of phenol onto AC, whereas in the current references, there is so far almost very little information on the results and analysis of the role of Fe doping in AC's structure and/or surface chemistry of AC, the phenol adsorption capacity and the mechanism of, desorption and oxidation of phenol over support AC and Fe/ACs, so it is very worth systematically studying whether phenol is effectively adsorbed, desorbed and oxidized on the adsorbent-catalysts.

In this work, Fe/ACs were prepared by wet pore impregnation and subsequently main influential experiment parameters such as contact time, initial phenol concentration, temperature and pH in phenol removal were studied. To describe the adsorption process, the equilibrium and thermodynamic data of the adsorption were investigated by different models. Furthermore, the information on various regeneration methods such as thermal regeneration and the phenol oxidation behavior was also given to study the catalytic role of Fe in the phenol oxidation process. In order to valuate reasonable regeneration technologies, the second adsorption capacity of the sorbent-catalysts for phenol in solutions after regenerations was also compared. To assess re usability of Fe/AC in the consecutive adsorption-oxidation runs, the adsorption capacities of Fe/AC for phenol in solutions after every cycle were finally compared.

2. Materials and methods

2.1. Adsorbate

Phenol as an adsorbate is of analytical grade. It was dissolved in distilled water to yield aqueous solutions at different concentrations.

2.2. Adsorptive-materials

A commercial coal-derived granular activated carbon (GAC) used as original material came from Xinhua Chemical Plant (Taiyuan, China). The GAC was crushed into particles of 40–60 meshes, washed by distilled water several times and dried at 110°C for 48 h. The resulting activated carbon was denoted as AC.

Fe-doping activated carbons (Fe/ACs) as adsorbent-catalysts were prepared by the following steps: 1) all pores of AC were impregnated with a $\text{Fe}(\text{NO}_3)_3$ solution at different concentrations, and then 2) the AC was aged at room temperature for 2 h, and dried in air at 50°C and at 110°C for 6 h, respectively; finally, 3) the samples were calcined in a fixed-bed tubular glass reactor of 30 mm in id and 500 mm in length in N_2 atmosphere (99.99% , 12 ml min^{-1}) at 260°C for 2 h. Fe/AC with 1 wt.% and 5 wt.% of Fe is denoted as Fe1/AC and Fe5/AC, respectively. The preparation process was described in the previous study [14].

The phenol-adsorbing Fe5/AC and AC used in TPO and TPD experiments were prepared in batch adsorption experiments. The process was as follows: 0.500 g Fe5/AC or AC was submerged in a 50 ml aqueous solution at initial

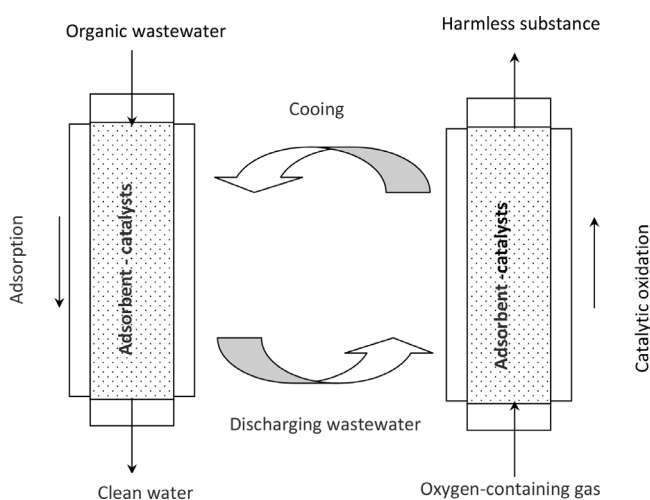


Fig. 1. Flow chart of adsorption-dry catalytic oxidation technology (ADCO) used for treating organic wastewater: adsorption, discharging, catalytic oxidation and cooling.

phenol concentration of 500 mg L⁻¹ in a 50 ml flask, which was continuously agitated by a thermostatic water-bath shaker at 30°C and 150 rpm for 12 h. The phenol-adsorbing samples were separated from the solution by a filtration method, and then dried in air at room temperature to a constant weight. The Fe5/AC and AC with phenol were termed Fe5/AC-phenol and AC-phenol, respectively. To investigate the role of Fe in Fe5/AC-Phenol, Fe5/AC-Blank and AC-Blank were also prepared after they were immersed in distilled water at the same preparation conditions as the phenol adsorption experiments.

2.3. Characterization

2.3.1. Chemical composition

Carbon (C), hydrogen (H), and nitrogen (N) contents of AC and Fe/ACs were determined by an element analyzer (Elementar Analysensysteme GmbH Vario EL), sulfur (S) content was analyzed by a sulfur analyzer (SC-132, LECO, USA), and oxygen (O) content was calculated by difference.

2.3.2. Texture

SEM-EDX data of AC and Fe/ACs were obtained using Hitachi S4800 scanning electron microscope (SEM). The information on pore structures of AC and Fe/ACs was obtained by liquid N₂ adsorption at 77K using an automatic ASAP 2020 volumetric sorption analyzer (Micromeritics, USA). Micro pore and mesopore volume of AC and Fe/ACs was calculated by t-plot. The specific surface area (S_{BET}) was calculated using the Brunauer–Emmett–Teller (BET) equation.

2.3.3. Surface chemistry characterization

In this work, surface functional groups of AC and Fe/ACs were qualitatively and quantitatively analyzed by Boehm titration, which was the same as the analysis method reported in the references [15,16]. Meanwhile, Fourier transform infrared spectroscopy (FTIR) [17] and temperature-programmed desorption (TPD) [18] were used to complement the experimental results from Boehm titration. FTIR analyses were performed in a Thermo Fisher iS10 Fourier transform infrared spectrometer (FTIR). The spectra were recorded from 4000 cm⁻¹ to 650 cm⁻¹. TPD profiles were obtained using a tubular quartz micro reactor of 6.0 mm in id and 370 mm in length inside an automatic electric furnace coupled with a quadrupole mass spectrometer (MS) (Balzers QMG 422, Switzerland). Each sample of 0.1000 g was heated in the reactor from room temperature to 800°C at a heating rate of 10°C/min under a flow of Ar (99.99%, 30 mL STP/min). CO₂ (m/e 44) and CO (m/e 28) desorbed from the adsorbents were monitored by MS.

To obtain the information on occurrence of Fe on the prepared Fe/AC, X-ray diffraction (XRD) patterns of the catalyst were obtained using Panalytical B.V X'Pert PRO equipped with Cu-Kα radiation source. The applied current and voltage were 40 mA and 40 kV, respectively. The sample was scanned over a 2θ range from 20 to 90° at a speed of 0.25° min⁻¹.

2.4. Batch adsorption

To investigate the adsorption behavior of AC or Fe/ACs for phenol from water, a series of batch experiments were carried out by changing the adsorptive conditions such as contact time, initial phenol concentration, pH and adsorption temperature. In the batch tests except contact time tests, the adsorption process was the same as the adsorption of phenol onto AC or Fe/ACs. It is noting that different initial concentrations (250, 500, 800, 1200, 1500, 2000, and 2500 mg L⁻¹), different temperatures (20°C, 30°C, 40°C and 50°C) and different pH (2, 5, 7.5, 10 and 12) were used, respectively. In contact time tests, agitation time for the experiments was various when maintaining other adsorption condition the same as the previous test.

After adsorption, the AC or Fe/ACs was separated from the solution by filtration and subsequently dried in air at room temperature. The concentration of the filtrate was determined using a 752N UV-Vis spectrophotometer (Shanghai Pudong optical instrument, China) at 270 nm, and the amount of phenol adsorbed on AC or Fe/ACs (q_e) was calculated by the following equations:

$$C = \frac{c}{m_1} \quad (1)$$

$$q_e = \frac{(C_i - C_e)V}{m_2} \quad (2)$$

where m_1 is molar mass of phenol (mg mmol⁻¹), and c and C are defined as mass concentration (mg L⁻¹) and molar concentration (mmol L⁻¹), respectively; V is solution volume (L), m_2 is mass of AC or Fe/ACs (g), and C_i and C_e are the initial phenol concentration (mmol L⁻¹) and equilibrium concentration (mmol L⁻¹), respectively.

2.5. Catalytic oxidation of phenol over Fe/AC

2.5.1. TPD behavior of phenol adsorbed on AC

To investigate thermo stability of AC-adsorbed phenol, TPD experiments of samples (AC-phenol and AC-blank) were carried out and products contained in outlet gas released in TPD were monitored by MS. Specific experiments were as follows: a sample of about 20 mg was placed in a tubular quartz reactor of 6 mm in id and 370 mm in length, and heated from room temperature to 600°C at 10°C min⁻¹ under a flow of 99.99% Ar (12 ml min⁻¹).

2.5.2. Catalytic oxidation of adsorbed phenol over Fe/AC

To obtain catalytic activity of the catalyst (Fe5/AC) and support (AC), temperature-programmed oxidation (TPO) experiment of Fe5/AC or AC was carried out, and weight loss and MS signals of products released in TPO were monitored in a TG-MS system. The TG apparatus is a SETSYS Evolution 16/18 analyzer (SETARAM), which is coupled with MS. A sample of about 20 mg was placed in the TG

and heated from room temperature to 600°C at 10°C min⁻¹ under a flow of 5% O₂/Ar (12 ml min⁻¹).

2.5.3. TPO of phenol on AC and Fe/AC with intermittent O₂ removal

To investigate the oxidation mechanism, TPO experiment of phenol on AC or Fe/AC with intermittent O₂ removal was carried out. The sample came from room temperature-dried filtration residue after AC or Fe/AC adsorbed 1400 mg/L phenol solutions.

2.6. Second adsorption of phenol onto AC and Fe/AC after various regenerations

To investigate changes in adsorption of phenol from solution onto AC or Fe/AC after different regeneration methods, second adsorption experiments in batch mode were carried out. The mentioned-above regeneration experiments included oxidation reaction and thermal regeneration. Phenol-adsorbing AC or Fe/AC was filtered and naturally dried to constant weight at room temperature after ending the adsorption of phenol at 2000 mg L⁻¹ or 1400 mg L⁻¹ at 30°C for 12 h. The sample placed in a fixed-bed tubular quartz reactor (6 mm id. and 370 mm in length) was heated from room temperature to certain temperature at a rate of 10°C min⁻¹ and maintained at this temperature under 5% O₂/Ar or 99.99% Ar at a flow rate of 80 ml min⁻¹ for a specific time. The second adsorption of Fe/AC or AC for phenol at certain concentration after the various regeneration were conducted in the same conditions as first one, and phenol uptake by AC or Fe/AC was calculated. Here, the sample was denoted as AC-XXX-XX-X-X or Fe/AC-XXX-XX-X-X: XXX, XX, X, X in sequence is denoted as constant regeneration temperature, specific time at this constant temperature, regeneration atmosphere type, regeneration number, respectively. AC and Fe/AC were represented as the original AC and Fe/AC before the first adsorption, respectively.

2.7. Reusability of Fe/AC for phenol removal in several runs

To investigate the stability of adsorption capacity of phenol onto Fe/AC in consecutive several runs, the adsorption experiments of Fe5/AC after each oxidation for phenol solution at 1400 mg/L were carried out in the other conditions same as the above batch experiments.

3. Results and discussion

3.1. Characterization of carbonic and Fe/ACs

SEM images of AC and Fe/ACs (Figs. 2a–c) show the external surface of AC and Fe/ACs has many irregular, spiral and different-pore-size pores and obviously the external surface of AC and Fe1/AC has more pore pores than that Fe5/AC. From EDX data (Figs. 2d–i), we observe that there is no element Fe and small amount of element O on AC surface, whereas Fe1/AC and Fe5/AC surface have higher Fe and O contents, and Fe and O contents of Fe1/AC are much lower than those Fe5/AC (Figs. 2d–i). The above results indicate that a decrease in pores of AC

and an increase in surface Fe and O contents occur after Fe(NO₃)₃ treatment. Fe/ACs contain lower C content than AC (Table 1), whereas, they have much higher Fe and O contents than AC (Table 1), which is in agreement with the above EDX results of AC and Fe/ACs. The Fe(NO₃)₃ treatment obviously increases O content of AC, which can be ascribed mainly to partial oxidation of element carbon during the doping treatment. As shown in Table 1 and Fig. 3, it is also easily seen that the differences in micro pore volume (V_{mic}) of the adsorbent-catalysts, most relevant to the adsorption capacity of organic compounds, are relatively small, indicating that the Fe(NO₃)₃ treatment has no major effect on AC texture. And a slight decrease in micro pore volume of Fe5/AC is attributed to AC's micro pore filling by element iron (possibly in ferric/ferrous oxides) or many oxygenated functional groups on the micro pore/mesopore of AC, which may block the access of nitrogen molecules into the micro pores. In Table 1, the basic groups of AC before and after Fe(NO₃)₃ treatment change slightly, but the surface acidic groups of Fe/ACs including carboxylic, lactonic, and phenolic groups are much more than those AC due to Fe(NO₃)₃ oxidation; furthermore, surface acidic groups of Fe/AC increase with an increase in Fe loading amount, which is in complete accord with the above-mentioned the trend for O content obtained by EDX and element analyses.

Obviously, AC and Fe/ACs have very similar FTIR spectra (Fig. 4). It is possible to observe that for Fe/ACs, especially Fe5/AC has the relatively strong IR bands related to adsorbed water (3000–3600 cm⁻¹) and surface functionalities with C=O (in carboxylic, anhydride, lactone and ketene at 1750–1630 cm⁻¹), C–O (lactonic, ether, phenol, etc. at 1300–1000 cm⁻¹), C–H (3100–2800 cm⁻¹), C–C (1600–1450 cm⁻¹) and C–H (3070–3030 cm⁻¹) in aromatic groups [19]. This indicates that more oxygen-containing groups have been introduced to AC surface after Fe(NO₃)₃ treatment, which is in agreement with the data of oxygen content shown in Fig. 2 and Table 1.

To further show the change in surface acidic groups of the mentioned-above adsorbents, TPD characterization technology was used, and CO₂ and CO released from the adsorbent-catalysts during TPD before 800°C were monitored by MS and the release curves are shown in Fig. 5. According to the fundamental principle of CO₂ and/or CO decomposed from surface oxygen-containing groups of AC at different characteristic temperatures in inert atmosphere upon heating [20], it can be seen that acidic groups (carboxylic acids, lactones, anhydrides and phenolic groups) of Fe/ACs are more than those AC, and acidic groups of Fe5/AC is much more than those Fe1/AC, which is in agreement with the data of oxygen content shown in Table 1 and Figs. 2 and 4. Therefore, we easily obtained that Fe(NO₃)₃ treatment obviously increases the surface acidic groups of AC.

To investigate occurrence of AC-supported Fe, XRD experiments were carried out. Fig. 6 shows only XRD pattern of Fe5/AC because of its low signal-to-noise ratio derived possibly from finely dispersed Fe-containing substances on support AC. The presence of Fe₂O₃ diffraction peaks and the low signal-to-noise ratio indicate that mainly Fe₂O₃ is finely dispersed on the AC surface. The same result was described in previous study [14].

3.2. Batch adsorption

3.2.1. Contact time

Contact time is an important parameter to determine the adsorptive time to reach thermal equilibrium state. Usually,

the characteristics of adsorbents and its available adsorption sites can affect the equilibrium time [21]. The experimental results for effect of contact time on phenol removal by AC and Fe/ACs are shown in Fig. 7. Like trends of q_t versus t [14], the adsorption curves of three samples for low-concen-

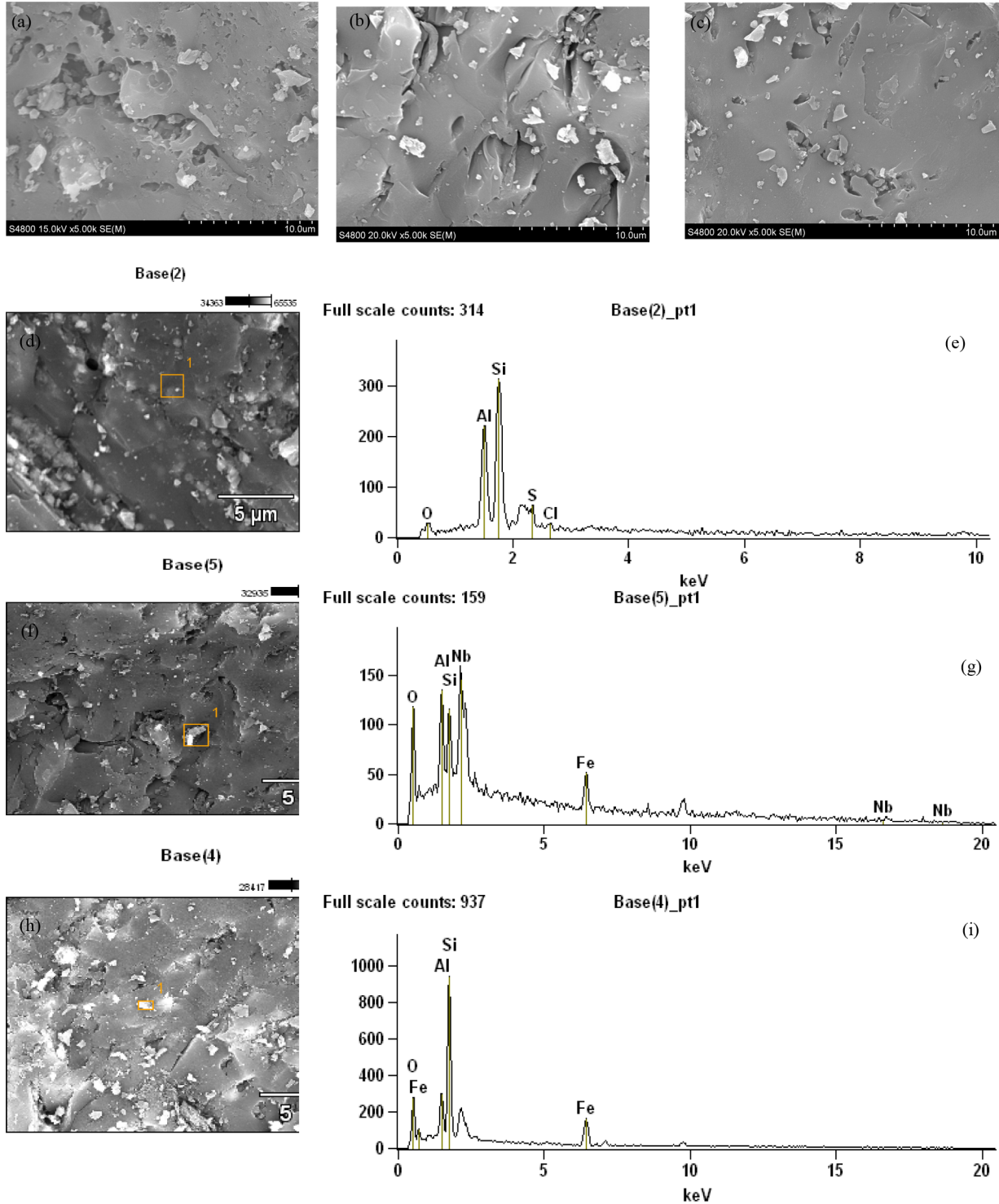


Fig. 2. SEM images and EDX of AC and Fe/ACs: (a) SEM images of AC; (b) SEM images of Fe1/AC; (c) SEM images of Fe5/AC; (d) and (e) SEM-EDX of AC; (f) and (g) SEM-EDX of Fe1/AC; (h) and (i) SEM-EDX of Fe5/AC.

Table 1
Composition, structure and surface chemical properties of AC and Fe/ACs (air-dried basis)

Adsorbents		AC	Fe1/AC	Fe5/AC
Elemental analyses	C_{ad} (wt%)	83.1	80.6	76.1
	H_{ad} (wt%)	1.19	1.23	1.30
	S_{ad} (wt%)	0.61	0.59	0.58
	N_{ad} (wt%)	0.65	0.61	0.58
	O_{ad} (wt%)	1.78	2.40	2.49
	Fe_{ad} (wt%)	0.38	1.26	5.04
	Lignition point (°C)	506.9	–	351.7
	Pore structures	V_{mic} (cm ³ /g)	0.204	0.204
V_{meso} (cm ³ /g)		0.318	0.311	0.288
S_{BET} (m ² /g)		916	899	845
Surface chemistry		Carboxylic (mmol/g)	0.010	0.074
	Lactonic (mmol/g)	0.132	0.173	0.318
	Phenolic (mmol/g)	0.077	0.208	0.299
	Surface acidity (mmol/g)	0.219	0.455	0.820
	Surface basicity (mmol/g)	0.672	0.588	0.682

Note: Surface acidity and surface alkalinity are the adsorbent-catalyst's surface acidic groups and surface basic groups, respectively.

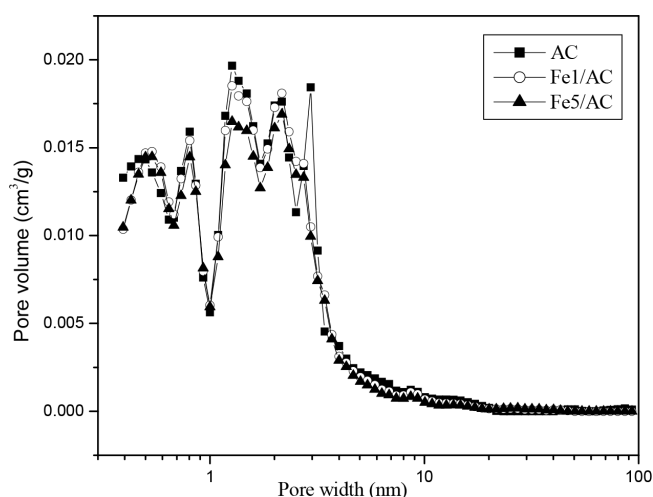


Fig. 3. Pore size distribution of AC and Fe/ACs.

tration phenol are obviously similar. The adsorption curves can be divided into three periods: rapid adsorption (before 120 min), slow adsorption and equilibrium periods (after equilibrium point). In the rapid adsorption period, large amounts of phenol are rapidly removed from solutions by AC and the catalysts, whereas in the equilibrium period the phenol removal percentage does not obviously change. The

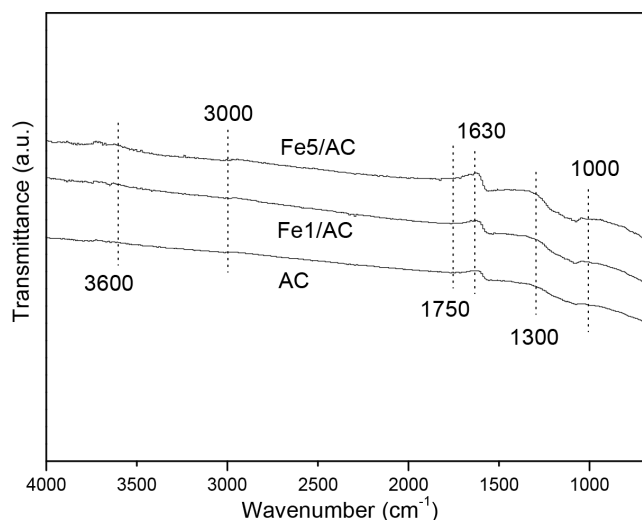


Fig. 4. FTIR spectra of AC and Fe/ACs.

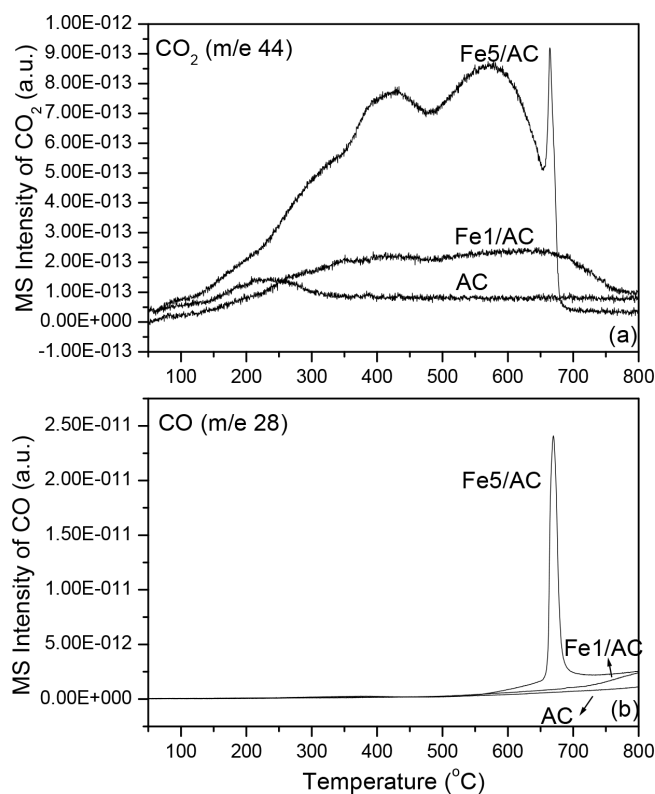


Fig. 5. TPD spectra of the adsorbents: (a) CO₂ evolution and (b) CO evolution.

phenol removal by the samples before adsorption equilibrium increases with an increase in contact time. However, adsorption curves of the samples for high-concentration phenol solutions like trends of q_t to t [14] are very different: 240 min (equilibrium time) for AC is obviously much less than 720 min for Fe1/AC and 360 min for Fe5/AC, which may be attributed to the thinner passage resulted from partial micro pore/mesopore filling directly by Fe doping or indirectly by many surface oxygenated groups of catalysts produced during doping. To ensure that adsorptions equi-

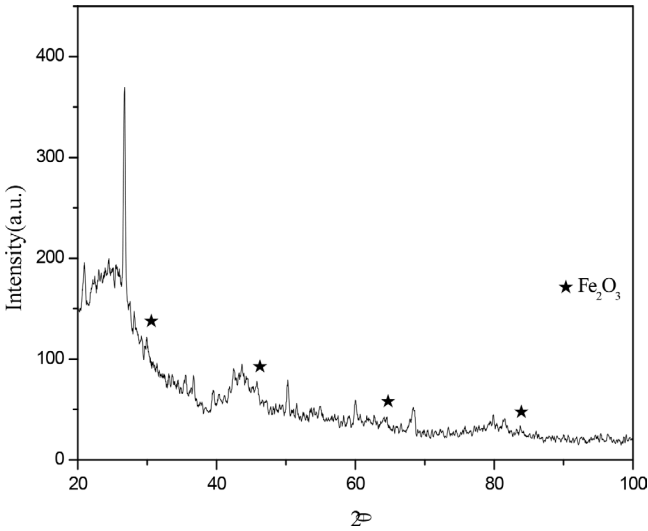


Fig. 6. XRD patterns of Fe5/AC.

librium is obtained, adsorptive processes in the following experiments were carried out for 12 h.

3.2.2. Initial concentration

The initial concentration of adsorbates provides an important driving force to overcome all mass transfer resistance of the adsorbates between the aqueous solution and solid phase. Due to the adsorption trends in other temperatures similar to those in 30°C, Fig. 8 shows merely the isothermal adsorption data of AC and Fe/ACs for phenol in the range of 250–2500 mg/L at 30°C. Generally, the trends for adsorption of phenol onto three samples are similar: all the equilibrium adsorption capacities of the samples for phenol increase rapidly with increasing initial phenol concentration, which can be ascribed from a rapid increase in initial driving force at solid/liquid interfaces. However, the

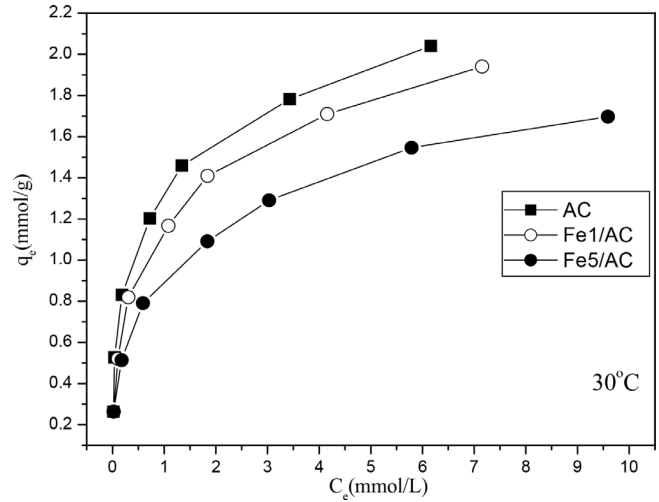


Fig. 8. Effect of initial phenol concentration on phenol uptake on AC and Fe/ACs at 30°C.

specific adsorption capacities of phenol onto AC and Fe/ACs are obviously different, i.e., for the same equilibrium concentration AC has the highest equilibrium uptake of phenol and Fe5/AC the lowest one, and the uptake of phenol by Fe/ACs decreases with increasing mass fraction of AC-supported Fe. This results indicate the $Fe(NO_3)_3$ treatment reduces the adsorption ability of AC for phenol from water, which has mainly its two possible adsorption-influencing reason, i.e., 1) physical structure and 2) surface chemistry of samples. Since the studied samples have the above-mentioned similar textures, their different adsorption behaviors can be clearly attributed only to the difference in surface chemistry. In this work, we only take into account that mainly surface acidic groups of the samples because alkaline Fe_2O_3 seem not to react with acidic phenol molecules. Based on the correlation of the surface acidic groups with equilibrium uptake of phenol, it can be read-

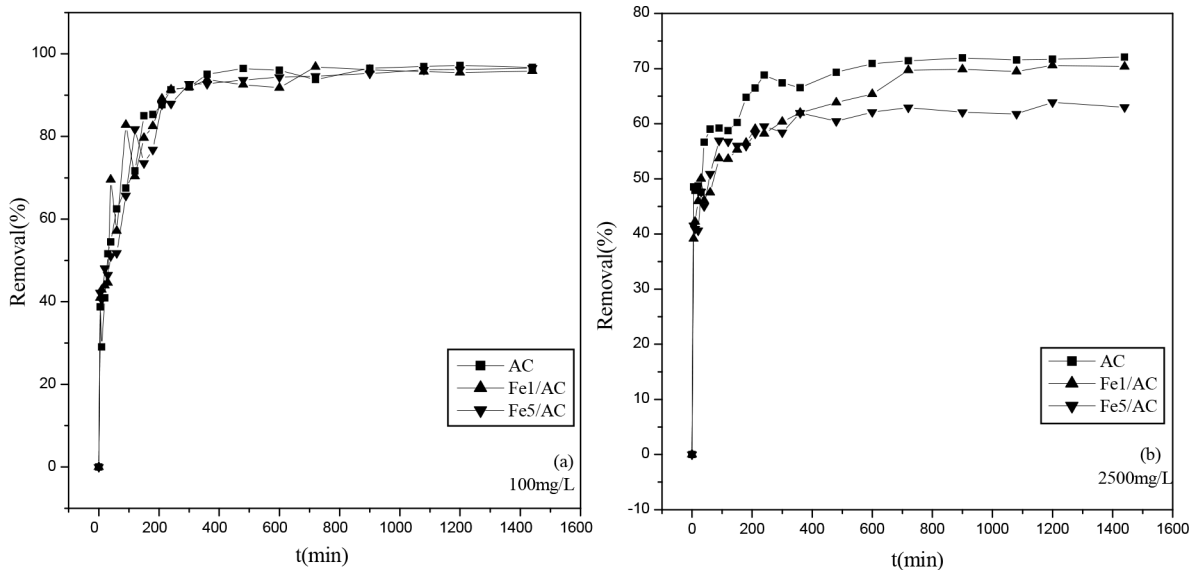


Fig. 7. Effect of contact time on phenol removal on AC and Fe/ACs: (a) 100 mg/L and (b) 2500 mg/L at 30°C.

ily concluded that the phenol uptakes by Fe/ACs decrease with an increase in surface acidic groups of Fe/ACs, which may be derived possibly from the adverse effect of AC-adsorbed water molecules.

When aromatic compounds molecules and water molecules coexist in a system, aromatic compounds are adsorbed mainly on the hydrophobic surface of AC due to non polarity of hexatomic ring of aromatics, whereas water molecules are adsorbed mainly on the polar surface because both water molecules and oxygenated groups are polar and H-bonds between water molecules and surface oxygenated groups (e.g., carboxylic acid) are formed [22]. According to the mechanism that more acidic surface groups of AC can increase more polar hydrophilic adsorption sites of AC and simultaneously reduce more nonpolar hydrophobic adsorption sites of AC because the $\text{Fe}(\text{NO}_3)_3$ treatment significantly increases surface acidic groups of AC, it is easily concluded that more water molecules are adsorbed on the oxygenated sites of Fe/AC in H-bond state, and finally decrease in the adsorption capacity of Fe/ACs for phenol. Furthermore, many water molecules adsorbed on AC surface may form water clusters in a 3D configuration [23], which can block the AC's pore passage, through which phenol molecules can pass into micro pores.

3.2.3. Adsorption temperature

Adsorption temperature is also an important influential parameter. The equilibrium adsorption data of phenol on the samples at 1200 mg L^{-1} at various temperatures (20°C , 30°C , 40°C and 50°C) are shown in Fig. 9. Clearly, the equilibrium phenol uptake by each samples decreases with adsorption temperature, indicating that an increase in experiment temperature is unfavorable for adsorption of phenol onto AC and Fe/ACs, which may be due to an increase in desorption rate of phenol from the surface of adsorbents into the aqueous solution at the high temperature.

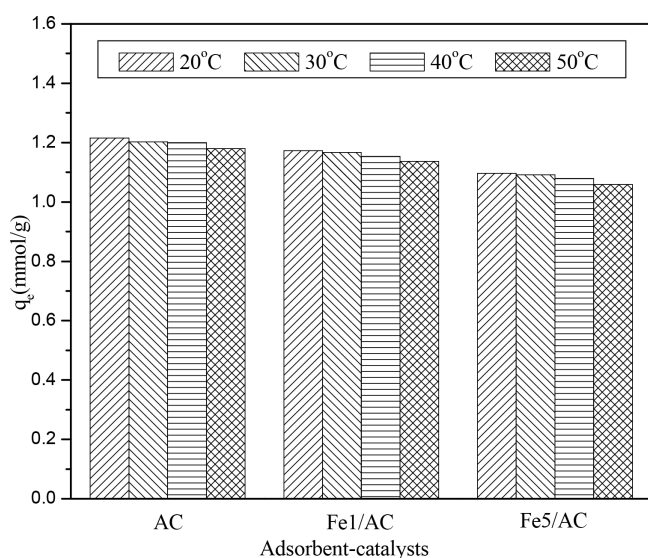


Fig. 9. Effect of temperature on phenol uptake on AC and Fe/ACs at initial concentration of 1200 mg/L .

3.2.4. pH

The adsorption data of phenol at 1200 mg L^{-1} onto the adsorbent-catalysts at various temperatures (2, 5, 7.5, 10 and 12) are shown in Fig. 10. Clearly, it is readily obtained that the trends for the effect of pH on the adsorption of phenol onto AC and Fe/ACs are similar (Fig. 10). Phenol uptake by each sample at $\text{pH} < 7.5$ slowly and slightly increases with pH, whereas the phenol uptake at $\text{pH} > 7.5$ quickly decreases with pH, indicating that the role of solution alkalinity in inhibiting the phenol removal by the samples is stronger than the acidity. Therefore, poor acidic and neutral condition is relatively appropriate for adsorbents removing phenol from solutions.

3.3. Adsorption isotherms

In this work, Langmuir, Freundlich, Dubinin-Radushkevich (D-R) and Temkin isotherm models were used to investigate the samples for phenol adsorption.

The Langmuir model, a mono layer adsorption model [24], which can be linearly expressed by

$$\frac{C_e}{q_e} = \frac{C_e}{Q_L} + \frac{1}{K_L Q_L} \quad (3)$$

where the meanings of q_e (mmol g^{-1}) and C_e (mmol L^{-1}) were the same as Eq. (2); Q_L (mmol g^{-1}) is the Langmuir parameter representing the saturation phenol adsorption capacity of the adsorbent; and K_L (L mmol^{-1}) is the Langmuir parameter related with the free energy of adsorption.

The Freundlich model, a frequently used empirical model [25], which is based on adsorption on heterogeneous surface. The model is represented by the following equation:

$$\ln q_e = \ln K_F + \frac{1}{n} \ln C_e \quad (4)$$

where K_F ($\text{mmol g}^{-1}(\text{L mmol}^{-1})^{1/n}$) and n as empirical constants are related with the adsorption capacity and the adsorption intensity, respectively.

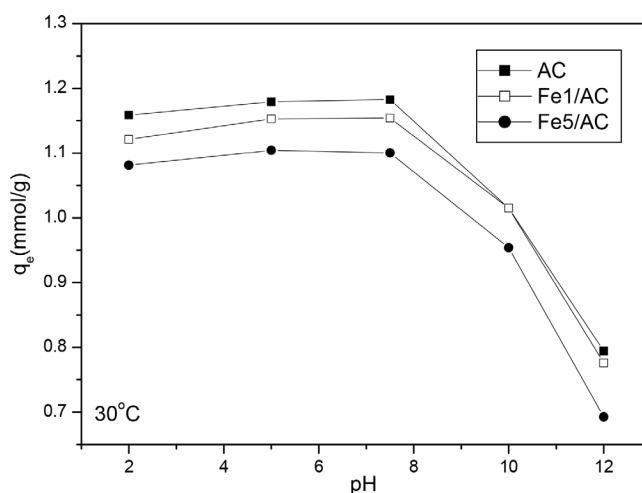


Fig. 10. Effect of pH on phenol uptake of AC and Fe/ACs at initial concentration of 1200 mg/L .

Not based on the assumption of a homogeneous surface or constant adsorption potential of AC, the Dubinin-Radushkevich model (D-R) is also a adsorption model to study the isotherms of a high degree of rectangularity [25]. This model is given by:

$$\ln q_e = \ln Q_{D-R} - \beta R^2 T^2 \ln^2 \left(1 + \frac{1}{C_e} \right) \quad (5)$$

$$T = t + 273.15 \quad (6)$$

where Q_{D-R} (mmol/g) is the theoretical saturation uptake, β ($\text{mol}^2 \text{kJ}^{-2}$) a constant is the average free energy of adsorption per molecule of the adsorbate when it is transferred to the surface of the solid from solution, R ($8.314 \text{J mol}^{-1} \cdot \text{K}^{-1}$) is the gas constant, and T (K) and t ($^{\circ}\text{C}$) are absolute temperature in Kelvin degree and experiment temperature in $^{\circ}\text{C}$, respectively.

Temkin model considers the adsorption heat of all the molecules in the layer decreases linearly with coverage due to interaction between adsorbate and adsorbent [26]. The model in linear form can be defined as follows:

$$q_e = F \ln K_T + F \ln C_e \quad (7)$$

where F is related with the adsorption heat, and K_T (L mmol^{-1}) as a constant is the maximum binding energy.

The experiment data of Fig. 8 were fitted by the above models, and the parameters of the models were calculated, and finally the parameters are listed in Table 2. Compared with the values of correlation coefficient (R^2), due to its higher correlation coefficient (both $R^2 = 0.977$), the Langmuir model better describes the experimental data of adsorption of phenol onto AC and Fe1/AC, indicating that AC and Fe1/AC have almost homogeneous nature of surface. The maximum phenol uptakes by AC and Fe1/AC reach $2.145 \text{ mmol g}^{-1}$ and $2.023 \text{ mmol g}^{-1}$, respectively. However, the Freundlich isotherm with its highest correlation coefficient ($R^2 = 0.991$) fits quite well with the experimental data of Fe5/AC. The fitting result shows that compared with AC and Fe1/AC, the Fe5/AC' surface has the stronger heterogeneous properties, which is mainly due to more ferric oxides and surface O-containing groups of AC introduced

after AC was treated by the high-mass-fraction $\text{Fe}(\text{NO}_3)_3$ solution.

3.4. Adsorption thermodynamics

To further understand the thermodynamic behavior, three important thermodynamic parameters such as Gibbs free energy change (ΔG°), enthalpy change (ΔH°) and the entropy change (ΔS°), which are often related with temperature of phenol in the adsorption process [21], were investigated. ΔG° of adsorption at various temperatures is calculated from the equations below:

$$\Delta G^{\circ} = -RT \ln K_e \quad (8)$$

where ΔG° (kJ/mol) is the Gibbs free energy change and K_e is an equilibrium constant, which can be calculated using:

$$K_e = \frac{q_e}{C_e} \quad (9)$$

According to Van't Hoff equation, ΔG° , ΔH° and ΔS° have the linear relation as Eq. (10):

$$\ln K_e = -\frac{\Delta G^{\circ}}{RT} = -\frac{\Delta H^{\circ}}{RT} + \frac{\Delta S^{\circ}}{R} \quad (10)$$

where ΔH° (kJ/mol) and ΔS° (J/kmol) are the enthalpy change and the entropy change, respectively. Values of ΔH° and ΔS° can be calculated from Eq. (10).

The above parameters calculated by Eq. (10) are shown in Table 3. All the negative values of the ΔG° at various temperatures indicate the phenol adsorption processes are spontaneous and feasible. Moreover, the absolute values of ΔG° increase with increasing temperature (Table 3), indicating that extent of the spontaneity of adsorption of phenol is proportional to the adsorption temperature. Interestingly, the absolute value of ΔG° at the same temperature (Table 3) decreases with an increase in mass fraction of AC-supported Fe, showing that the spontaneous nature of adsorption of phenol onto the samples is inversely proportional to the mass fraction of doped Fe, so it is concluded that to some extent the $\text{Fe}(\text{NO}_3)_3$ treatment thermodynamically inhibits adsorption of phenol from solutions. All the negative ΔH° values indicate

Table 2
Isotherm constants for the adsorption of phenol onto AC and Fe/ACs at 30°C

Isotherms	Adsorbents			Isotherms	Adsorbents		
	AC	Fe1/AC	Fe5/AC		AC	Fe1/AC	Fe5/AC
Langmuir				Freundlich			
Q_L (mmol/g)	2.145	2.023	1.805	K_F ((mmol/g) · (L/mmol) ^{1/n})	1.136	1.029	0.866
K_L (L/mmol)	2.162	1.681	0.962	n	3.052	3.158	3.506
R^2	0.977	0.977	0.982	R^2	0.959	0.972	0.991
D-R				Temkin			
Q_{D-R} (mmol/g)	1.580	1.605	1.373	K_T (L/mmol)	74.25	139.7	34.60
β	2.7×10^{-8}	2.8×10^{-8}	3.0×10^{-8}	F	0.3251	0.2614	0.2781
R^2	0.791	0.875	0.829	R^2	0.976	0.9670	0.978

Table 3
Thermodynamic parameters for the adsorption of phenol onto AC and Fe/ACs

t (°C)		20	30	40	50
ΔG° (KJ/mol)	AC	-2.964	-3.036	-3.108	-3.180
	Fe1/AC	-2.866	-2.932	-2.997	-3.063
	Fe5/AC	-2.707	-2.754	-2.801	-2.849
ΔH° (KJ/mol)	AC	-0.8544			
	Fe1/AC	-0.9448			
	Fe5/AC	-1.323			
ΔS° (J/Kmol)	AC	7.195			
	Fe1/AC	6.555			
	Fe5/AC	4.723			
R ²	AC	0.958			
	Fe1/AC	0.974			
	Fe5/AC	0.987			

that the adsorption of phenol from solution on samples are exothermic, which theoretically verifies the conclusion that equilibrium uptake of phenol from aqueous solution by the samples decreases with temperature. Interestingly, the absolute value of ΔH° of the samples increases with an increase in Fe content of Fe/AC (Table 3). All the positive values of the ΔS° suggest an increase in randomness at the solid/solution interface in the adsorption of phenol on the samples.

3.5. Regeneration of phenol-adsorbing AC and Fe/AC

3.5.1. TPD behavior of phenol-over AC

To obtain thermostability of phenol adsorbed on AC surface, products released from AC-phenol and AC-blank during TPD were monitored in MS while TPD experiments were carried out, and the MS curves of products are shown in Fig. 11. It can be obtained that: 1) before about 250°C and after about 400°C, the curve of phenol released from AC-Phenol is similar to that AC-Blank, whereas between about 250°C and 400°C AC-Phenol starts to deviate from AC-Blank (Fig. 11a), indicating that desorption of phenol from AC surface occurs in the range of about 250°C to 400°C during TPD; 2) H₂O release curve can be separated into two parts (Fig. 11b): similar H₂O curves of both AC-Phenol and AC-Blank before about 150°C are derived from evaporation of water adsorbed on AC; water released at the temperature higher than 150°C may be derived from dehydrolysis of phenol on AC; 3) some benzene are released between about 250°C and about 400°C in TPD (Fig. 11c), which could be ascribed to partial decomposition of phenol over AC; 4) the other phenol-related organic compounds such as cyclohexane, cyclohexanone, hexalin, and quinone are not detected during TPD (Figs. 11d–g). Therefore, we conclude that in heating process AC-adsorbed phenol is mainly desorbed from AC surface and simultaneously the decomposition and/or polymerization of some phenol also occur, showing that AC surface-adsorbed phenol has poor thermostability like the results in the reference [6]. However, the heating method also provides a thermal regeneration method to

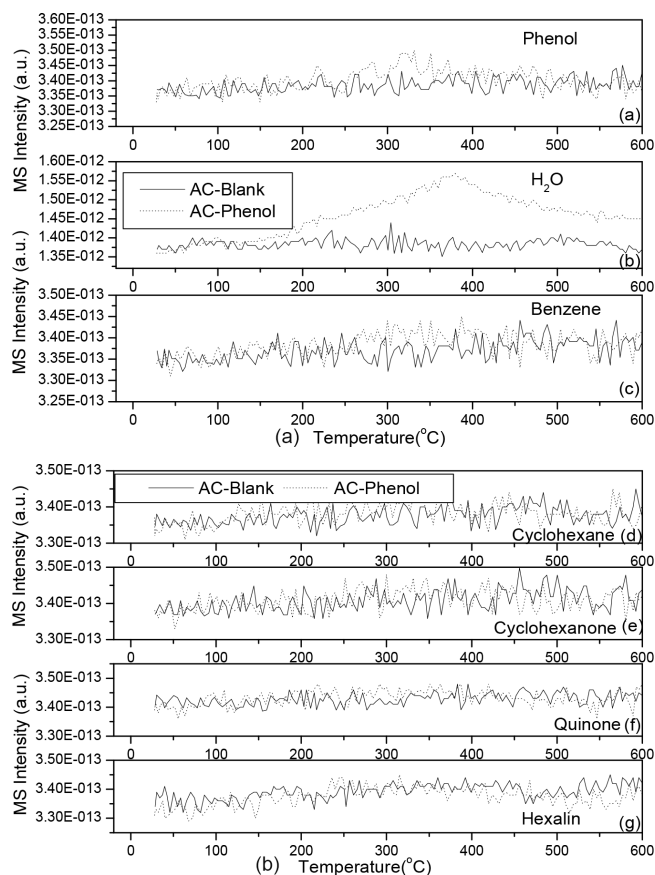


Fig. 11. MS spectra of products released from phenol on AC in TPD: AC-Blank (solid) and AC-Phenol (dot).

resume AC's phenol capacity after adsorption of phenol onto AC terminates. Unfortunately, due to their high toxicity, the main products (phenol and benzene) released in TPD must be treated again before discharging, but the second treatment mode will greatly increase the treatment cost.

3.5.2. TPO behavior of phenol over Fe/AC

Fig. 12 shows TG/DTG-MS curves of AC-Blank and AC-Phenol during TPO. The weight losses of AC-blank and AC-phenol before 463.2°C and 484.2°C respectively are slow and minor, but after the two temperatures, weights of AC-Blank and AC-Phenol quickly decline (Fig. 12a), which is accompanied by O₂, CO₂ and H₂O released (Figs. 12b and c), indicating that AC or organic compounds quickly are oxidized. In the range of 182.5°C and 295.5°C, DTG curve of AC-Phenol deviates from that AC-Blank, and reaches a minimum value at 238°C, which corresponds to release of some extra water and some phenol, and meanwhile no other phenol-related compounds (benzene, cyclohexane, cyclohexanone, hexalin, and quinone) is not detected (Figs. 12d–e), which can be ascribed to polyreaction of phenol molecules on AC surface. Beyond 295.5°C water is also released, which can be ascribed possibly to polyreaction of new organic molecules on AC surface. Therefore, it is easily obtained that during TPO, AC has almost insignificant ability of catalytic oxidation of AC surface-adsorbed phenol

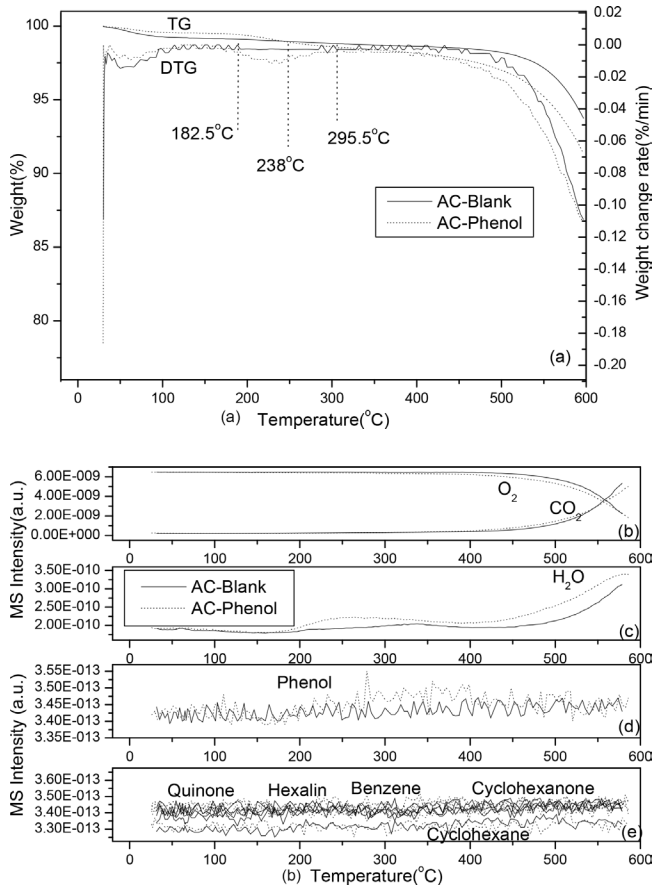


Fig. 12. TG/DTG-MS profiles for TPO of AC-Blank (solid) and AC-Phenol (dot): (a) TG/DTG and (b) and (c) MS spectra of products released in oxidation of phenol.

like the results of AC in the references [6,7], but the phenol and phenol-related degradation products or some polymers strongly deposit on AC surface.

To study catalytic oxidation behavior of phenol on Fe/AC, TPO experiments of Fe5/AC-phenol and Fe5/AC-Blank were carried out in TG-MS. TG profile of Fe5/AC-phenol starts to deviate from that of Fe5/AC-Blank at around 221.5°C and a peak occurs at 310°C (Fig. 13a). The weight loss recorded for this peak in the temperature range of 221.5–351.7°C is about 3.7wt%. After subtracting weight loss of Fe5/AC itself in the same temperature range, a net weight loss of Fe5/AC-Phenol is about 1.7wt%, which corresponds to 34.7% of total amount of Fe5/AC-adsorbed phenol. It can be observed in Fig. 13b that before 221.5°C, CO₂ released from Fe5/AC-phenol is similar to that Fe5/AC-Blank, whereas at about 221.5°C it starts to quickly deviate from Fe5/AC-blank, then reaches a plateau at 310°C, and finally slowly rises from 310°C to 351.7°C. From Fig. 13b, the above-generated CO₂ is accompanied by great O₂ consumption, which corresponds to the significant weight loss of Fe5/AC-phenol (Fig. 13a), showing that element C in phenol molecules adsorbed on Fe5/AC is oxidized into CO₂. Furthermore, it is also obtained that an initial oxidation temperature of phenol over Fe/AC and an initial ignition temperature of AC are 221.5°C and 351.7°C, respectively. In addition, H₂O released in Fig. 13c can be separated

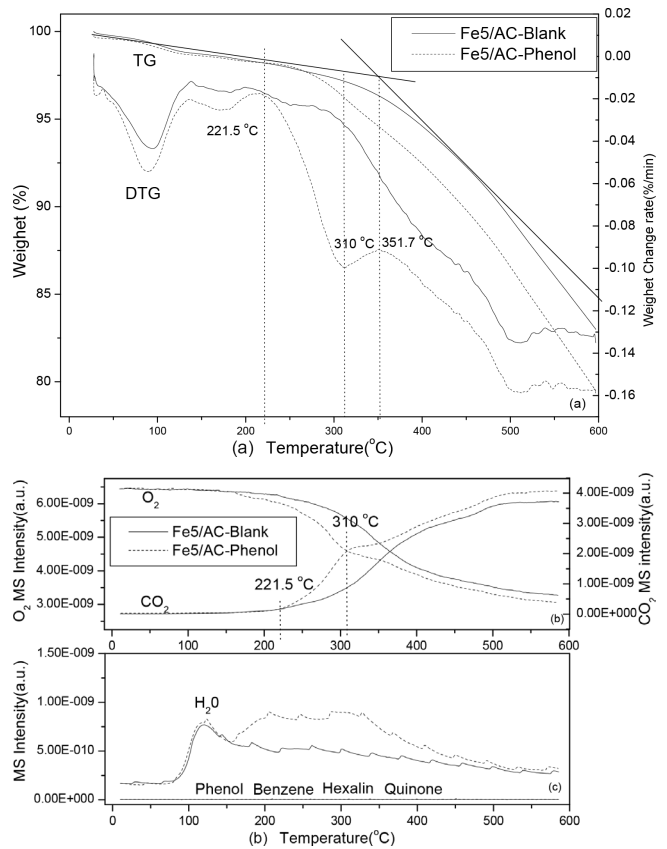
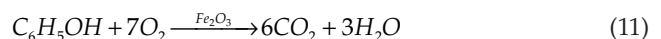


Fig. 13. TG/DTG-MS profiles for TPO of Fe5/AC-Blank (solid) and Fe5/AC-Phenol (dot): (a) TG/DTG and (b) and (c) MS spectra of products released in oxidation of phenol.

into three parts: similar H₂O release curves of both Fe5/AC-Phenol and Fe5/AC-Blank before 150°C are resulted from evaporation of Fe5/AC-adsorbed water during heating; water released between 150°C and 221.5°C may be derived from the partial polymerization of phenol on the catalyst; water released beyond 221.5°C corresponds to CO₂ produced during TPO, which can be ascribed to the oxidation of element H in phenol over Fe5/AC. It should be noted that there are no other organic compound molecules including benzene and phenol released in TPO (Fig. 13c). The experiments results indicate that Fe5/AC-adsorbed phenol seems to be completely oxidized into CO₂ and H₂O at a temperatures window of 221.5–351.7°C in TPO, which is similar to the phenol oxidation behavior over Fe/AC [5–7], but the temperatures window of phenol oxidation by Fe₂O₃ of Fe/AC in this work is obviously wider than that by magnetic Fe₃O₄ of Fe/CMK-3 [5]. The total oxidation reaction of phenol over Fe/AC is as follows:



3.5.3. TPO of phenol over AC and Fe/AC with intermittent O₂ removal

To further study how Fe₂O₃ works in catalytic oxidation of phenol, transient reaction experiments in TPO were conducted and the results are shown in Fig. 14. Fig. 14a shows

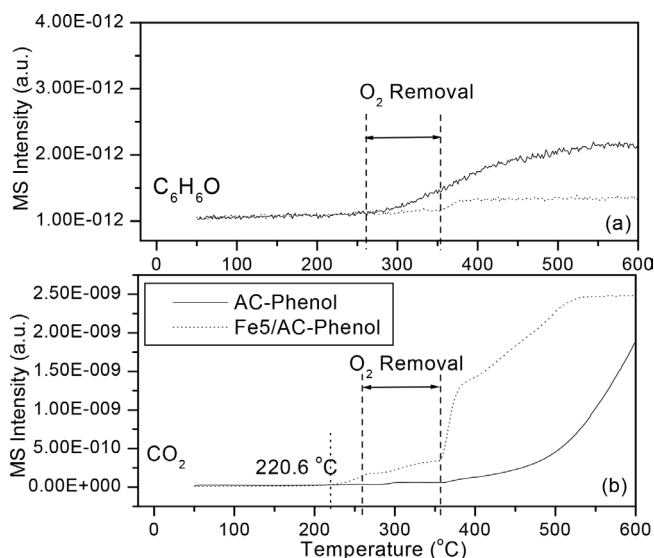
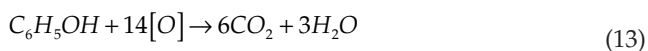


Fig. 14. MS profiles during TPO of phenol loaded (11.8%) over AC and Fe5/AC with intermittent O₂ removal.

that from about 260°C Fe₂O₃ doped on Fe/AC obviously inhibits desorption of phenol from AC surface. Furthermore, it is also found that between about 220.6°C and about 260°C, MS spectrum of CO₂ of Fe5/AC under O₂ flow (dot line) begins to deviate from that AC (solid line), which can be ascribed to the oxidation of phenol by O₂, whereas in the range of about 260°C to 355°C, the difference in MS spectra of CO₂ of Fe5/AC (dot line) and AC (solid line) with intermittent O₂ removal is obvious (Fig. 14b). The difference is also still derived from the oxidation of phenol over Fe/AC, but element oxygen needed in the latter phenol oxidation is resulted only from covalent oxygen atoms of Fe₂O₃ on Fe/AC surface due to no O₂ molecules in gas. According to the analysis of the catalytic role of CeO₂ and Fe(II)/Fe(III) described in the references [27,28], the possible phenol oxidation mechanism is speculated as follows:



Some active radical [O] may be released from AC-supported Fe₂O₃ [Eq. (12)], a large amount of AC-adsorbed phenol molecules may be oxidized into CO₂ and H₂O by the active [O] as described in Eq. (13) and reductive FeO may be oxidized into Fe₂O₃ by oxidant O₂ [Eq. (14)], which is continuously used to be active species of catalyst in catalytic run.

From the analysis above, it is deduced that while Fe₂O₃ of Fe/AC surface has high catalytic oxidation performance of Fe/AC-adsorbed phenol, the oxidation may simultaneously resume its fresh adsorption sites of Fe/AC for phenol, which contributes to recycling use of the Fe/AC in ADCO and finally obviously decrease the catalyst cost.

Compared to those rigorous ones for wet air oxidation of phenol (at 5 MPa, 200°C) [29,30] and those for thermal desorption of phenol (normal atmosphere, about 700°C), the light-duty experimental conditions (normal atmosphere, about 250°C) for the dry catalytic oxidation of phenol over Fe/AC (ACDO) can be easily realized in labs or even in industries. Furthermore, there are no pollutants released in ADCO while catalysts can oxidize phenol into CO₂ and H₂O. Therefore, ADCO is technically feasible for dilute phenol-containing wastewater treatment even if the Fe/AC suffers some weight loss due to partial oxidation of AC.

3.6. Second adsorption of phenol on AC and Fe5/AC after regenerations

In order to investigate the adsorption stability of AC and Fe5/AC for phenol after different regenerations, second adsorption experiments were carried out and the phenol uptakes of AC and Fe/AC were calculated. Various, the uptake of phenol by AC and Fe5/AC changes with different regenerations (Fig. 15): 1) second adsorption capacity of ACs regenerated at each temperature all lower than original AC, and for the same regeneration time, the uptakes increase with increasing thermal regeneration temperature, showing that the higher temperature is favorite to restore the ability of AC to adsorb phenol from solutions; 2) at the same thermal regeneration temperature, second adsorption capacity of ACs increase with the regeneration time, indicating that the longer regeneration time is helpful to restore the phenol uptake by AC; 3) in the same other regeneration conditions, second adsorption capacity of AC regenerated in Ar is higher than that in O₂/Ar, which may be derived from some adsorption sites occupied by more polymerisates of AC-adsorbed phenol under O₂; 4) the uptake of Fe5/AC for phenol solution at 2000 mg/L is much lower than that AC owing to more surface oxygenated groups of Fe/AC, whereas the sec-

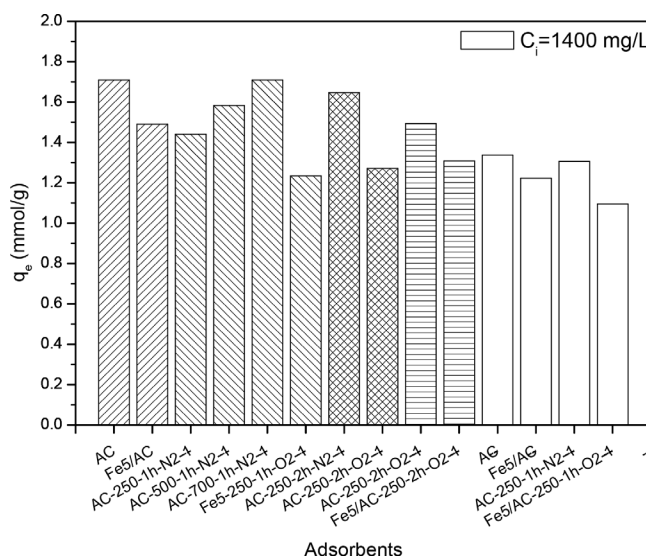


Fig. 15. Uptake of phenol on adsorbents at 30°C after thermal regeneration or catalytic oxidation.

ond capacity of different regeneration time-regenerated Fe5/AC for phenol solution at 2000 mg/L also is lower than that Fe5/AC possibly owing to some large-molecule organic residues produced because of the incomplete oxidation of phenol in oxidation process [6]; furthermore, the uptake of phenol solution at 2000 mg/L by Fe5/AC regenerated for 2 h is slightly higher than that for 1 h, indicating that longer time is conducive to catalytically oxidize phenol; 5) the second 1400 mg/L-phenol uptake by Fe5/AC is also lower than that Fe5/AC. And hence the conclusion can be drawn that only for second adsorption capacity, i.e. uptake recovery, traditional thermal regeneration of phenol-adsorbing AC significantly superior to dry catalytic oxidation of phenol over Fe/AC, whereas on the other hand thermal regeneration also inevitably produces and releases a large amount of very toxic pollutants (phenol and benzene)-containing off-gas (Fig. 11), which will seriously pollute ambient air and finally endanger the organisms. Therefore, other purification facilities such as absorption column or reaction column must be installed after thermal regeneration equipment, which unfortunately greatly enhances complexities of techniques and treatment cost and resultantly seriously limits the applicable range of the thermal regeneration. Compared with the thermal generation, it has lower phenol uptake, but Fe/AC can efficiently oxidize Fe/AC-adsorbed phenol into some pollution-free compounds such as carbon dioxide and water, and has higher second phenol uptake, so only for green treatment of phenol, dry catalytic oxidation is significantly superior to thermal regeneration.

3.7. Adsorption of phenol onto Fe/AC in several adsorption-oxidation runs

It is important for the adsorbent-catalysts to have high removal reusability in several runs, so the adsorption tests of phenol onto Fe5/AC in consecutive adsorption-oxidation runs were carried out and the results are shown in Fig. 16. Various, phenol uptake by Fe5/AC quickly decreases with adsorption-oxidation runs before 8th cycle, after which the uptake does not almost change and still amounts to

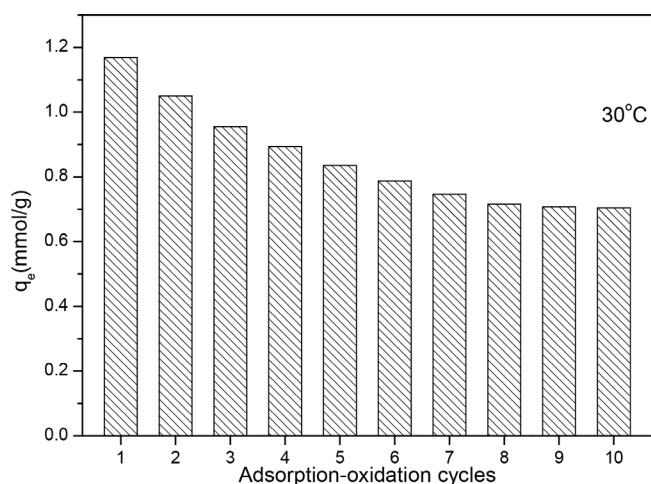


Fig. 16 Uptake of phenol at 1400 mg/L by Fe5/AC at 30°C in the consecutive runs.

60.7% of initial uptake. It is worthy of noting that the ratio of 10th uptake to initial uptake by Fe/AC is obviously higher than that Cu5/AC [1], that Cu5-Ce1/AC [6] and that AC [31], indicating that the reusability of Fe/AC in phenol adsorption capacity is obviously superior to Cu5/AC, Cu5-Ce1/AC and AC [1,6,31]. It should be noted that the phenol uptake by Fe5/AC after 10 cycles is still similar to the initial uptake by Fe/CMK-3 in the reference [5]. And if the specific adsorption process that 0.5 g adsorbent deals with 50 mL of 1000 mg/L phenol can be used as a basis for the comparison of percent phenol removal by unit-mass Fe5/AC in this work and that by Fe5/CMK-3 in the reference [5], it is easily found that Fe5/CMK-3 obviously has the lower phenol initial removal percentage (merely 60% removal) than Fe5/AC (90% for initial removal) and even much lower than 80.1% for Fe5/AC to remove 1400 mg/L phenol. It shows that Fe/CMK-3 in the reference seems not to be efficient for the removal of higher-concentration phenol due to its poor initial phenol capacity. The decrease in uptake after many cycles may be ascribed to carbon loss or some polymers formed during oxidation process [6], the specific mechanism of which needs to be further studied in next work.

4. Conclusions

It does not significantly change pore structure of AC; but ferric nitrate treatment obviously increase the surface acidic groups (mainly surface acidic oxygen-containing groups such as carboxylic groups, phenolic hydroxyl groups, and lactone groups) of AC. Adsorptive removal percentages of phenol from water by AC and Fe/AC increase with the contact time and phenol concentration, respectively, whereas phenol removal decreases with increasing temperature. At the same equilibrium concentration, the order of equilibrium uptake is AC > Fe1/AC > Fe5/AC due to the adverse effect of many water molecules adsorbed on surface hydrophilic sites of AC and/or many water clusters produced to hinder the access of phenol molecules into micro pores.

Langmuir model can better describe adsorption of phenol onto AC and Fe1/AC (AC doped with low-mass-fraction Fe) due to almost homogeneous surface, but for Fe5/AC (high-mass-fraction Fe-doping AC), Freundlich model can quite well describe adsorption process due to its surface heterogeneity. The trends of effect of pH on adsorption of AC and Fe/ACs are similar. For each adsorbent, phenol uptake, prior to pH of 7.5, slowly and slightly increases with pH, whereas phenol uptake at pH > 7.5 quickly decreases with pH. Phenol removal by AC and Fe/AC is spontaneous and exothermic. Thermal regeneration can desorb phenol from AC. Compared with AC, Fe/AC has high catalytic oxidation activity of phenol and the oxidation can resumes adsorption sites of Fe/AC for phenol from solution. Fe/AC after 10 adsorption-catalytic oxidation cycles still has higher phenol uptake. For clean phenol treatment, the dry catalytic oxidation method is significantly superior to thermal regeneration.

The stated-above results indicate that activated carbons-based Fe binary functional adsorbent-catalyst having liquid-phase adsorption of phenol and dry catalytic oxidation activity of phenol can be used to effectively treat phenol-containing wastewater.

Acknowledgements

The authors express their grateful appreciation for the financial support from the Research Project Supported by Shanxi Scholarship Council of China (No. 2014-059), National Natural Science Foundation of China (No. 21576277), the Undergraduate Innovation and Training Program Fund of Shanxi province (No. 2016280) and the Doctorate Science Fund of Taiyuan University of Science & Technology (No. 20182057).

Symbols

AC	— Power activated carbon in 40–60 meshes
AC-Blank	— H ₂ O-adsorbing AC
AC-Phenol	— Phenol-adsorbing AC at initial phenol concentration of 1200 mg/L
c [mg L ⁻¹]	— Phenol mass concentration
C [mmol L ⁻¹]	— Phenol molar concentration
C_i and C_e [mmol L ⁻¹]	— Initial and equilibrium molar concentrations of phenol in solution, respectively
F	— Temkin parameter related with the adsorption heat
Fe1/AC	— AC doped with 1 wt% of iron
Fe5/AC	— AC doped with 5 wt% of iron
Fe5/AC-Blank	— H ₂ O-adsorbing Fe5/AC
Fe5/AC-Phenol	— Phenol-adsorbing Fe5/AC at initial concentration of 2000 mg/L
FeO	— Product after AC-supported Fe ₂ O ₃ is reduced by phenol
Fe ₂ O ₃	— AC-supported Fe ₂ O ₃ after AC is treated by Fe(NO ₃) ₃
GAC	— Coal-derived granular activated carbon
K_e	— Thermodynamic constant
K_F [(mmol g ⁻¹) (L mmol ⁻¹) ^{1/n}]	— Freundlich parameter related with the adsorption capacity
K_L [L mmol ⁻¹]	— Langmuir parameter related with the free energy of adsorption
K_T [L mmol ⁻¹]	— Temkin parameter related with the maximum binding energy
m_1 [mg mmol ⁻¹]	— Molar mass of phenol
m_2 [g]	— Adsorbent mass
n	— Freundlich parameter related with the adsorption intensity
q_e [mmol g ⁻¹]	— Equilibrium capacity of an adsorbent for phenol
Q_L [mmol g ⁻¹]	— Langmuir parameter representing the maximum phenol adsorption capacity on an adsorbent
Q_{D-R} [mmol g ⁻¹]	— D-R parameter representing the theoretical saturation uptake
R [8.314] (mol·K) ⁻¹	— Gas constant
t [°C]	— Adsorption temperature in Celsius degree
T [K]	— Absolute temperature
V [L]	— The solution volume
β [mol ² kJ ⁻²]	— D-R parameter representing the mean free energy of adsorption per

molecule of an adsorbate when it is transferred to the surface of the solid from infinity in the solution

ΔG° [kJ mol ⁻¹]	— Gibbs free energy change
ΔH° [kJ mol ⁻¹]	— Enthalpy change
ΔS° [J (k mol) ⁻¹]	— Entropy change
[O]	— Active oxygen

References

- [1] J. Zhao, Z. Liu, D. Sun, TPO-TPD study of an activated carbon-supported copper catalyst-sorbent used for catalytic dry oxidation of phenol, *J. Catal.*, 227 (2004) 297–303.
- [2] F. Herrera, A. Lopez, G. Mascolo, P. Albers, J. Kiwi, Catalytic decomposition of the reactive dye Uniblue A on hematite: modeling of the reactive surface, *Water Res.*, 35 (2001) 750–760.
- [3] L. Hu, S. Dang, X. Yang, Incorporation of CuO into mesoporous carbon CMK-3 and its adsorption and catalytic oxidation of phenol, *Acta Phys. Chim. Sin.*, 26 (2010) 373–377.
- [4] R. Fang, H. Huang, J. Ji, M. He, Q. Feng, Y. Zhan, D. Y.C. Leung, Efficient MnOx supported on coconut shell activated carbon for catalytic oxidation of indoor formaldehyde at room temperature, *Chem. Eng. J.*, 334 (2018) 2050–2057.
- [5] L. Hu, S. Dang, X. Yang, J. Dai, Synthesis of recyclable catalyst-sorbent Fe/CMK-3 for dry oxidation of phenol, *Micropor. Mesopor. Mater.*, 147 (2012) 188–193.
- [6] Z. Lei, Z. Liu, Behavior of Cu-Ce/AC catalyst-sorbent in dry oxidation of phenol, *Fuel Process. Technol.*, 88 (2007) 607–615.
- [7] L.N. Prodan, A.M. Koganocski, V.I. Kofanov, Catalytic regeneration of activated carbon saturated with surface active agents, dyes and phenol, *Khim. Tekhnol. Vody.*, 10 (1988) 278–283.
- [8] E. Lorenc-Grabowska, M.A. Diez, G. Gryglewicz, Influence of pore size distribution on the adsorption of phenol on PET-based activated carbons, *J. Colloid Interf. Sci.*, 469 (2016) 205–212.
- [9] A.M. Carvajal-Bernal, F. Gómez, L. Giraldo, J.C. Moreno-Piraján, Adsorption of phenol and 2,4-dinitrophenol on activated carbons with surface modifications, *Micropor. Mesopor. Mater.*, 209 (2015) 150–156.
- [10] G.S. dos Reis, M.A. Adebayo, C.H. Sampaio, E.C. Lima, P.S. Thue, I.A.S. de Brum, S.L.P. Dias, F.A. Pavan, Removal of phenolic compounds from aqueous solutions using sludge-based activated carbons prepared by conventional heating and microwave-assisted pyrolysis, *Water Air Soil Poll.*, 228 (2017) 1–17.
- [11] P. Kowalczyk, A. Deditius, W.P. Ela, M. Wiśniewski, P.A. Gauden, A.P. Terzyk, S. Furmaniak, J. Włoch, K. Kaneko, A.V. Neimark, Super-sieving effect in phenol adsorption from aqueous solutions on nanoporous carbon beads, *Carbon*, 135 (2018) 12–20.
- [12] A. Dasgupta, J. Matos, H. Muramatsu, Y. Ono, V. Gonzalez, H. Liu, C. Rotella, K. Fujisawa, R. Cruz-Silva, Y. Hashimoto, M. Endo, K. Kaneko, L.R. Radovic, M. Terrones, Nano structured carbon materials for enhanced nitrobenzene adsorption: Physical vs chemical surface properties, *Carbon*, 139 (2018) 833–844.
- [13] M. Ondarts, L. Reinert, S. Guittonneau, S. Baup, S. Delpeux, Jean-Marc Lévêque, L. Duclaux, Improving the adsorption kinetics of ibuprofen on an activated carbon fabric through ultrasound irradiation: Simulation and experimental studies, *Chem. Eng. J.*, 343 (2018) 163–172.
- [14] B. Li, K. Sun, Y. Guo, J. Tian, Y. Xue, D. Sun, Adsorption kinetics of phenol from water on Fe/AC, *Fuel*, 110 (2013) 99–106.
- [15] N.A. Khan, H.J. An, D.K. Yoo, S.H. Jung, Polyaniline-derived porous carbons: Remarkable adsorbent for removal of various hazardous organics from both aqueous and non-aqueous media, *J. Hazard. Mater.*, 360 (2018) 163–171.
- [16] X. Zheng, H. Lin, Y. Tao, H. Zhang, Selective adsorption of phenanthrene dissolved in Tween 80 solution using activated carbon derived from walnut shells, *Chemosphere*, 208 (2018) 951–959.

- [17] B. Li, Z. Lei, X. Zhang, Z. Huang, Adsorption of simple aromatics from aqueous solutions on modified activated carbon fibers, *Catal. Today*, 158 (2010) 515–520.
- [18] S.A. Messele, O.S.G.P. Soares, J.J.M. Órfão, C. Bengoa, F. Stüber, A. Fortuny, A. Fabregat, J. Font, Effect of activated carbon surface chemistry on the activity of ZVI/AC catalysts for Fenton-like oxidation of phenol, *Catal. Today*, 240 (2015) 73–79.
- [19] V.M. Gun'ko, V.V. Turov, O.P. Kozynchenko, D. Palijczuk, R. Szmigielski, S.V. Kerus, M.V. Borysenko, E.M. Pakhlov, P.P. Gorbik, Characteristics of adsorption phase with water/organic mixtures at a surface of activated carbons possessing intra particle and textural porosities, *Appl. Surf. Sci.*, 254 (2008) 3220–3231.
- [20] I.I. Salame, T.J. Bandoz, Surface chemistry of activated carbons: combining the results of temperature-programmed desorption, Boehm and potentiometric titrations, *J. Colloid Interf. Sci.*, 240 (2001) 252–258.
- [21] M. Kilic, E. Apaydin-Varol, A.E. Pütün, Adsorptive removal of phenol from aqueous solutions on activated carbon prepared from tobacco residues: Equilibrium, kinetics and thermodynamics, *J. Hazard. Mater.*, 189 (2011) 397–403.
- [22] N. Wibowo, L. Setyadhi, D. Wibowo, J. Setiawan, S. Ismadji, Adsorption of benzene and toluene from aqueous solutions onto activated carbon and its acid and heat treated forms: Influence of surface chemistry on adsorption, *J. Hazard. Mater.*, 146 (2007) 237–242.
- [23] A. Dąbrowski, P. Podkościelny, Z. Hubicki, M. Barczak, Adsorption of phenolic compounds by activated carbon—a critical review, *Chemosphere*, 58 (2005) 1049–1070.
- [24] M.A. Islam, I.A.W. Tan, A. Benhouria, M. Asif B.H. Hameed, Mesoporous and adsorptive properties of palm date seed activated carbon prepared via sequential hydrothermal carbonization and sodium hydroxide activation, *Chem. Eng. J.*, 270 (2015) 187–195.
- [25] K.C. Bedin, A.C. Martins, A.L. Cazetta, O. Pezoti, V.C. Almeida, KOH-activated carbon prepared from sucrose spherical carbon: Adsorption equilibrium, kinetic and thermodynamic studies for Methylene Blue removal, *Chem. Eng. J.*, 286 (2016) 476–484.
- [26] A.C. Martins, O. Pezoti, A.L.C. azetta, K.C. Bedi, D.A.S. Yamazaki, G.F.G. Bandoc, T. Asefa, J.V. Visentainer, V.C. Almeida, Removal of tetracycline by NaOH-activated carbon produced from macadamia nut shells: Kinetic and equilibrium studies, *Chem. Eng. J.*, 260 (2015) 291–299.
- [27] Z. Lei, Study of Cu-Ce/AC catalyst–sorber for treating phenol-containing wastewater by adsorption-catalytic dry oxidation [Doctoral thesis], Graduate School of Chinese academy of Science, 2007.
- [28] K. Rusevova, F. Kopinke, A. Georgi, Nano-sized magnetic iron oxides as catalysts for heterogeneous Fenton-like reactions—Influence of Fe(II)/Fe(III) ratio on catalytic performance, *J. Hazard. Mater.*, 241–242 (2012) 433–440.
- [29] K. Fajerweg, H. Debellefontaine, Wet oxidation of phenol by hydrogen peroxide using heterogeneous catalysis Fe-ZSM-5: a promising catalyst, *Appl. Catal. B - Environ.*, 10 (1996) 229–235.
- [30] Y. Yan, S. Jiang, H. Zhang, Catalytic wet oxidation of phenol with Fe-ZSM-5 catalysts, *RSC Adv.*, 6 (2016) 3850–3859.
- [31] J. Zhao, Study of AC-supported metals catalyst–sorber for treating phenol-containing wastewater by adsorption-catalytic dry oxidation [Doctoral thesis], Graduate School of Chinese academy of Science, 2003.